STM JOURNALS

Journal of
Power Electronics & Power Systems

https://journals.stmjournals.com/jopeps

ISSN: 2249-863X (Online)
ISSN: 2321-4244 (Print)
Volume 14, Issue 3, 2024
September–December
DOI (Journal): 10.37591/JoPEPS

Research JoPEPS

Hydrogen Storage System for Household Installation

Carlos Armenta-Déu*

Abstract

In this work, we study domestic renewable energy installations using compressed gaseous hydrogen as a storage system. The article analyzes the suitability and feasibility of this installation type considering energy, technical, and security aspects. The proposed configuration represents an alternative to the classical storage energy system in batteries, reducing dependence on grid supply for a negative balance of self-power generation to energy consumption. The hydrogen storage system is valid for any household installation, provided a specific safe place is available. Compressed hydrogen reduces the tank size but increases the risk of explosion, thus forcing us to reinforce the security measurements. The simulation run for an installation prototype shows that a hydrogen tank of 150 liters operating in the range from 0 to 70 bars, stores enough energy to maintain a null dependence on the energy grid. The system shows the advantage of having a flexible energy storage capacity, which adjusts through the tank pressure. The energy storage capacity range depends on the tank pressure tolerance, which depends on the tank material. The simulated system operates within a 25% extra capacity range, higher than any battery storage system.

Keywords: Autonomous system, energy balance, household installation, hydrogen storage, renewable energies, self-consumption

INTRODUCTION

Modern trends to reduce grid dependence in household installations promote self-consumption through autonomous renewable energy systems, such as photovoltaics [1]. Because solar radiation is intermittent and depends on meteorological conditions, the balance between power generation and energy consumption may result in positive, negative, or null values [2]. For negative balance, grid connection or storage system dependence is mandatory. Currently, the grid connection has a power supply limited by the grid line capacity, whereas the storage energy capacity depends on the system topology [3]. The current storage system is a battery block, lead-acid, or lithium type, whose energy capacity depends on the battery block size and configuration; the optimization of battery size reduces the null energy balance [4].

Energy storage in batteries suffers from continuous degradation, which reduces its energy capacity over time [5], thus limiting household installation autonomy and increasing its dependence on grid connections [6]. The battery storage capacity should match the negative peak value throughout the year to avoid grid dependence. However, this configuration increases battery size and cost, which causes user rejection [7].

Small residential batteries (3–5 kWh) are designed for self-consumption of electricity, including peak-demand shaving and time-of-use shifting [8, 9]. People who worry about missing excess energy when photovoltaic generation exceeds energy consumption select this configuration; the alternative option to battery block installation is the so-called virtual battery, which is

*Author for Correspondence
Carlos Armenta-Déu
E-mail: cardeu@fis.ucm.es

Faculty of Physics, Department of Matter Structure, Thermal Physics and Electronics, Complutense University of Madrid, Madrid, Spain

Received Date: August 10, 2024
Accepted Date: August 25, 2024
Published Date: September 18, 2024

Citation: Carlos Armenta-Déu. Hydrogen Storage System for Household Installation. Journal of Power Electronics & Power Systems. 2024; 14(3): 22–40p.

nothing but an energy exchange with the grid [10]. However, a virtual battery has the advantage of no energy capacity limits compared to the classical battery block.

Virtual batteries are becoming popular among PV system householders as a replacement for the battery block because they reduce investment and maintenance costs and represent a compensating method for excess energy when PV generation exceeds energy consumption [11]. However, virtual batteries suffer from local and national regulations and private company policies, which may impose restrictions on energy exchange between the household power system and grid or low compensation prices for the energy excess [12].

Hydrogen storage is an alternative to the use of battery blocks or virtual battery systems. An energy storage system based on hydrogen is flexible and energy-storage capacity adapted [13] and avoids grid dependence. Although hydrogen storage technology is well known, it is applied to vehicles [14] and large installations [15]. Until now, few commercial household energy storage systems based on hydrogen exist [16–19]; therefore, this configuration type allows for deeper development.

In this work, we propose implementing a hydrogen storage unit as a reservoir system to absorb the excess energy from a household PV installation and deliver the stored energy when power requirements exceed PV generation. The prototype uses a compressed hydrogen tank as a storage unit with pressure as the relevant parameter to establish the system energy capacity, thus providing flexibility to the operational mode and enlarging the energy capacity within the technological setup limits. The proposed prototype represents a novelty in the household energy storage field and a challenge for implementing hydrogen storage technology in domestic residences.

THEORETICAL FOUNDATIONS

Chemical storage uses excess electrical energy to produce compounds and store them conveniently. When required, these products are converted back into electricity. The compounds considered for storage are hydrogen and hydrocarbons such as methane or synthetic gasoline. The advantage of these compounds is their higher energy density compared to other storage systems, such as mechanical storage systems. Among them, hydrogen is the most efficient and feasible because it can be produced directly from renewable energy, whereas the other compounds are derived from hydrogen and a carbon source [20].

The physical and chemical properties of hydrogen make it particularly suitable for domestic energy storage. The principal characteristics are listed below.

- Light and abundance
- Highly flammable
- Low volumetric energy density
- High mass-energy density
- Colorless, odorless, and tasteless

Owing to these properties, hydrogen requires little space for storage if compressed at adequate pressure, but it should be handled carefully because of its high flammability.

Hydrogen produces energy in two ways: through fuel cells and combustion. In the latter, hydrogen reacts with oxygen to produce water and energy according to the following equation:

$$H_2 + \frac{1}{2}O_2 \rightarrow H_2O + Q \quad (1)$$

Where, Q = 286 kJ/mole = 0.08 kWh/mole [21].

Applying the hydrogen molecular mass, we have combustion energy per mass unit.

$$\xi^{o}_{comb} = 4.41\ kWh/kg(H_2) \quad (2)$$

Molecular hydrogen production is achieved by electrolysis or reformation. Electrolysis requires water while reforming requires hydrocarbons. At the industrial level, both processes are feasible, but in domestic residences, hydrogen generation should be produced by electrolysis because the reforming process requires between 400°C and 800°C [22].

Molecular hydrogen produced by electrolysis requires the energy generated by the PV system on a building rooftop. The electrolysis energy value is 237.13 kJ/mole of water, equivalent to 237.13 kJ/mole of hydrogen because electrolysis generates one hydrogen mole per mole of water (Equation (3)).

$$H_2O \rightarrow H_2 + \frac{1}{2}O_2 \tag{3}$$

Now, applying the hydrogen molecular mass once again:

$$\xi_{ely} = 32.9\ kWh/kg(H_2) \tag{4}$$

The energy efficiency of the electrolysis/combustion process was poor at 13.4%. Nevertheless, because the energy for electrolysis is free, as it comes from the solar panels, the only cost is the compression work, which is expressed as

$$W = \frac{m_{H_2}}{\rho_{H_2}}\Delta P \tag{5}$$

m_{H_2} and ρ_{H_2} are the hydrogen mass and density, and ΔP is the pressure gain.

Considering the compression work and combustion power, we define the COP as:

$$COP = \frac{\xi^o_{comb}}{W} = \frac{\rho_{H_2}\xi^o_{comb}}{m_{H_2}\Delta P} \tag{6}$$

Replacing value from Equation (2) and using the hydrogen density [23]:

$$COP = \frac{1.429x10^6}{\Delta P} \tag{7}$$

Equation (7) shows that the COP decreases as the pressure increases. Representing the COP versus the pressure gain (Figure 1), we notice that the COP quickly lowers for pressure gains up to 30 bar, and then reduces slowly until it remains almost constant from pressure to 100 bar.

Because the hydrogen density, and thus the mass, depends on pressure, the combustion power for a pressurized tank is.

$$\xi_{comb} = \xi^o_{comb}\frac{V_{tk}\rho^o_{H_2}}{\dot{m}_{H_2}}\frac{P_{tk}}{P_{atm}} \tag{8}$$

V_{tk} and P_{tk} are the hydrogen tank volume and pressure, respectively. Super-index *o* for hydrogen density corresponds to ambient pressure, P_{atm}

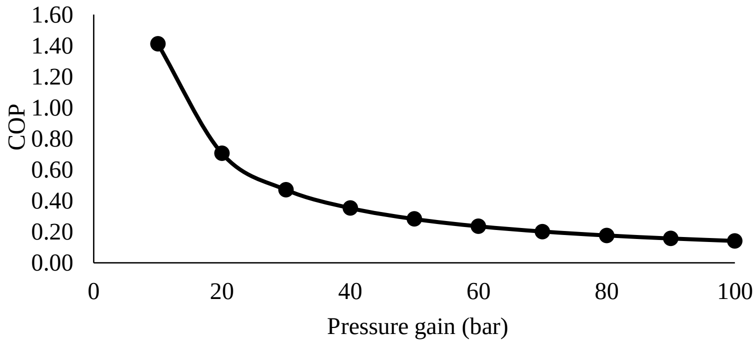

Figure 1. Theoretical evolution of COP with pressure gain.

On the other hand, the hydrogen compression requires a power given by:

$$\dot{W}_{comp} = \frac{\dot{m}_{H_2}}{\rho^o_{H_2}} \Delta P \quad (9)$$

Gas compression produces heat, which increases the gas temperature. For a constant volume, such as in a compressed hydrogen tank, the Boyle-Mariotte law applies. Therefore,

$$\frac{P}{T} = \frac{P^o}{T^o} \quad (10)$$

P^o and T^o represent the ambient pressure and temperature, respectively, and P and T correspond to the final pressure and temperature in the gas tank after compression, respectively.

The heating rate in a gas tank depends on the compression time, considering the hydrogen tank immersed in water at a constant temperature, and applying the heat conduction differential equation [24]:

$$m_{gas} c_{gas} \frac{dT_{gas}}{dt} = -\frac{\kappa_w A}{e}\left(T_{gas} - T_w\right) \quad (11)$$

Because m_{gas} changes with time, considering hydrogen as an ideal gas, Equation (11) is converted into.

$$V_{gas} c_{gas} \frac{d(PT)_{gas}}{dt} = -\frac{\kappa_w A}{e}\left(T_{gas} - T_w\right) \quad (12)$$

The sub-indexes *gas* and *w* account for hydrogen and water; *c* and *T* are the hydrogen-specific heat and absolute temperature, respectively; and *A*, *κ*, and *e* are the tank area, thermal conductivity, and thickness, respectively.

Solving Equation (12):

$$(PT)_{gas} = (PT)_w + [(PT)_{amb} - (PT)_w]e^{-at} \quad (13)$$

With:

$$a = \frac{\kappa A}{e V_{gas} c_{gas}} \quad (14)$$

Solving for t in Equation (13):

$$t = -\frac{1}{a} ln\left[\frac{(PT)_{gas} - (PT)_w}{(PT)_{amb} - (PT)_w}\right] \quad (15)$$

Replacing $(PT)_{gas}$ from Equation (10):

$$t = -\frac{1}{a} ln\left[\frac{P^2_{gas} T_{amb} - P^2_{amb} T_w}{P^2_{amb}(T_{amb} - T_w)}\right] \quad (16)$$

Operating at constant ambient pressure and temperature and considering that the water temperature remains constant, Equation (16) is converted into.

$$t = -\frac{1}{a} ln\left[\frac{P^2_{gas} T_{amb} - A}{B}\right] \quad (17)$$

With:

$$A = P^2_{amb} T_w \; ; \; B = P^2_{amb}(T_{amb} - T_w) \quad (18)$$

Applying the first derivative to Equation (17), equaling to zero for the maximum condition and operating

$$\Delta t_{max} = \frac{2}{a} T_{amb} \frac{P_{gas}\left(P_{gas} - P_{amb}\right)}{P^2_{gas} T_{amb} - P^2_{amb} T_w} \quad (19)$$

Equation (19) provides suitable time for hydrogen compression as a function of the final pressure, P_{gas}, minimizing the heating rate, and maintaining the gas temperature.

Now, applying Equations (9):

$$\dot{W}^{o}_{comp} = \frac{\rho_{H_2} V_{tk}}{\rho^{o}_{H_2} \Delta t_{max}} \left(P_{gas} - P^{o}\right) \quad (20)$$

ρ_{H_2} represents the compressed hydrogen density.

Since the compressor does not work ideally:

$$\dot{W}_{comp} = \frac{\dot{W}^{o}_{comp}}{\eta_{comp}} = \frac{1}{\eta_{comp}} \frac{\rho_{H_2} V_{tk}}{\rho^{o}_{H_2} \Delta t_{max}} \left(P_{gas} - P^{o}\right) \quad (21)$$

Where η_{comp} represents compressor efficiency, and the super-index *o* for the power accounts for ideal operating conditions.

Equation (21) shows the power required from the PV panels to compress hydrogen. Therefore, the global PV power P^{o}_{FV}, is:

$$P^{o}_{FV} = \dot{W}_{comp} + V_{op} I_{max} \quad (22)$$

V_{op} is the operating voltage, and I_{max} is the peak current of electrical appliances and accessories.

Considering energy losses and DC-AC converter efficiency, η_{conv}:

$$P_{FV} = \frac{\dot{W}_{comp} + V_{op} I_{max} + I^{2}_{DC} R_{FV}}{\eta_{conv}} + I^{2}_{ac} R \quad (23)$$

The sub-indexes AC and DC account for alternate and direct current, respectively, and R_{FV} and R are the line resistances from the PV panels to the converter and from the converter to the home electric board meter, respectively.

We calculated the energy balance ξ_{net} in the system using the following expression:

$$\xi_{net} = P_{FV}(psh) - V_{op} \sum_{i=1}^{n} I_i t_i - I^{2}_{DC} \left(R_{FV} + V_r^{2} \eta^{2}_{conv}\right) t_{op} \quad (24)$$

V_r represents the voltage ratio at the converter, V_{DC}/V_{AC}, and t_{op} is the operation time.

If the energy balance is positive, excess energy is used in the electrolyzer to produce hydrogen.

HOUSEHOLD INSTALLATION CHARACTERISTICS

We selected a semi-detached house with a 238 m^2 living area and a 70 m^2 basement for parking, a workshop, and a storage room. The living area was divided into three floors: low-level, main floor, and attic. The parking zone has a reserved area for heating and hot water tanks, a thermal comfort control system and accessories, a space for batteries, an electrolyzer, and a water tank containing a hydrogen tank.

The household installation has a global power of 8.84 kW. Because the panels are oriented east–west, we calculated the power generation for a south orientation, resulting in a value of 6.63 kW. The household installation had a grid input power limitation of 5.5 kW for an operating voltage of 220 V_{AC}. The maximum current is 25 A. The PV panels connect to the electric mainframe, so the household installation has a maximum power of 12.13 kW.

The peak power demand was 10.92 kW, considering the simultaneity factor for all appliances and accessories; therefore, the maximum allowed power was above the peak power demand by 11.1%. The standard power demand depends on the thermal comfort unit because it is the most consuming element; when the aerothermal equipment is working, the standard power demand is 5.125 kW; otherwise, it is 4.125 kW. According to these values, the household installation may operate on a PV system or grid on sunny or cloudy days.

The household installation is located near the city of Madrid (Spain) with a yearly average value of the peak sun time of 4.21 hours; however, to be more accurate, the monthly peak sun time is provided in Table 1 [25]. Household installation is automated to avoid excessive power demand; if the power demand exceeds the power limit, the control system automatically disconnects the consuming element to reduce the power demand below the limit. The element selection follows a setup pattern according to element relevance; the fridge never disconnects.

Design Layout

Hydrogen production and storage systems consist of a PV system as a power source, a double DC/AC, and an AC/DC converter to adapt the supplied DC voltage from PV panels, an electrolyzer, a compressor, a hydrogen tank, and a water container. Other accessories such as voltage and current, energy, and hydrogen flow meters are part of the hydrogen system. We used a K-type thermocouple attached to the hydrogen tank surface and immersed it in a hydrogen tank and water container to determine the temperature.

The PV system consists of 22 panels of 36.2 V output voltage and 11.1 A maximum output current for an output power of 401.8 W. Two strings of 11 panels in series each are connected in parallel; each parallel line generates 398.2 VDC for a total power of 4420 W. The two power lines supplied a maximum output power of 8840 W.

The hydrogen tank, with a capacity of 150 liters capacity, was built into stainless steel to avoid hydrogen losses and to favor thermal energy transfer to water. A pressure gauge measured the hydrogen pressure inside the tank, and when the pressure reached the maximum setup value, the control system opened a relay and disconnected the DC/DC converter from the PV power, interrupting the power supply to the electrolyzer and hydrogen production.

The household mainframe supplied an alternate current to operate the distilled water pump and hydrogen compressor. The control unit commands the commuter, relays for the water distiller pump, and DC/AC and AC/DC converters. We used a double converter, DC/AC, and AC/DC, because there is no single converter from 400 V_{AC} to 12 V_{DC}.

We show a schematic representation of the operational system in Figure 2. We replaced the fuel cell with a hydrogen burner to save money because fuel cells are expensive and require maintenance. Figure 1 does not include a hydrogen burner because it is similar to a gas burner with no technical relevance for this study.

SIMULATION

We consider three energy consumption configurations, low, medium, and high-power demand, characterized by their peak powers of 2961 W, 6080 W, and 10372 W. Every configuration corresponds to a consumption element distribution and includes all elements that operate simultaneously.

The simulation was run on sunny days to make the PV system available as a power source. We used the monthly peak sun hours listed in Table 1 to simplify the calculation. We assume that on cloudy days, the household installation runs on a grid power supply, and the hydrogen storage system is useless.

We based the simulation analysis on the energy balance between photovoltaic generation and household installation consumption because the excess energy, if any, is used to generate hydrogen at the electrolyzer, thus allowing the storage of the produced hydrogen.

ISSN: 2249-863X (Online), ISSN: 2321-4244 (Print)

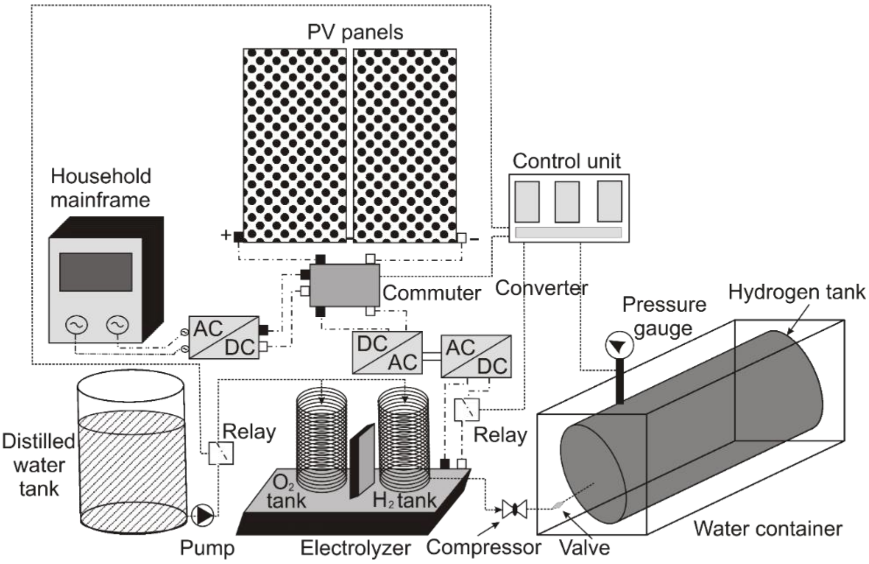

Figure 2. Schematic view of the operational system.

Table 1. Monthly peak sun hours for the location of Madrid (Spain).

J	F	M	A	M	J	J	A	S	O	N	D
4.55	5.02	5.62	6.25	6.79	7.06	6.93	6.47	5.86	5.24	4.69	4.40

The energy balance calculation is based on the daily period. Although it simplifies the calculation, it reduces the accuracy, as all days are assumed to be equal for the selected month. Nevertheless, it is a common practice when dealing with renewable energy sources, such as solar photovoltaics.

Because the energy demand changes according to human needs and habits, which depend on the period of the year, we should establish a pattern for the energy demand throughout the year; to that goal, we establish three periods for the year, according to the monthly energy demand [26]. These three periods correspond to July and August (high-power demand), December through March (medium-power demand), September through November, and April to June (low-power demand).

Energy Balance

The daily solar photovoltaic generation is derived from the monthly peak sun hours and the maximum solar radiation for clear-sky days [27] as follows:

$$\xi_{FV} = \eta_{conv}^{DC-AC} \eta_{conv}^{AC-DC} N P_{FV} (psh) f_\gamma \quad (25)$$

N is the number of PV panels, P_{FV} is the panel peak power, η_{conv} is the converter efficiency, and f_γ is the azimuth correction factor due to the east-west panel orientation. Super-index DC-AC and AC-DC–DC converter efficiencies account for the continuous-to-alternate conversion and vice versa.

For the prototype household installation, the DC/AC and AC/DC converter efficiencies are 0.975 [28] and 0.93 [29], respectively. The maximum inverter power is 3000 W because the electrolyzer consumes 1538.5 W and its efficiency is 75%, thus requiring an input power of 2051 W [30].

The daily average solar photovoltaic energy depends on the time of the year since the peak sun hours are different for every month. Considering the peak sun hours from Table 1, a variable number of panels from 4 to 22 in 2-step intervals, the efficiency of the converters, the individual PV panel peak power (P_{FV}=401.8 W), and the azimuth correction factor (f_γ=0.75) (Figure 3).

The selection of panel numbers is based on the premise that they should be installed in pairs because of the rooftop orientation, east-west, which forces this configuration to maintain power generation

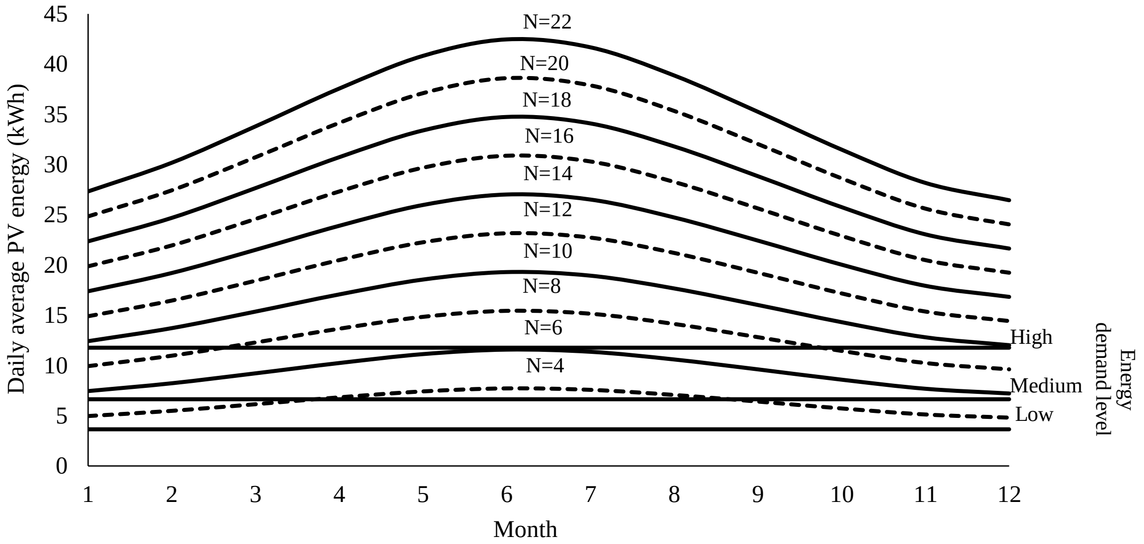

Figure 3. Monthly daily average PV generation and household energy demand.

Table 2. Daily average energy demand.

Power level demand	**Low**	**Medium**	**High**
Energy demand (kWh)	3.650	6.640	11.773

balance throughout the day. The minimum number is set to four because it is the standard default number for semi-detached and detached houses; the top number of 22 corresponds to the maximum available rooftop coverage factor. The horizontal solid lines correspond to the average daily household energy demand levels: low, medium, and high.

The average daily household energy consumption depends on the time of use of each appliance or device. Considering the three proposed configurations, low, medium, and high-power demand, 2961 W, 6080 W, and 10372 W, respectively, and the hourly distribution of daily usage, the average energy demand is determined (Table 2). We established the daily energy balance by comparing the photovoltaic generation and energy demand. The results of the calculations are shown in Figures 4–6.

Each bar group corresponds to the same panel distribution, starting at 22 panels to 14 panels, following the sequence 22, 20, 18, 16, and 14 panels. This configuration applies to Figures 4–12.

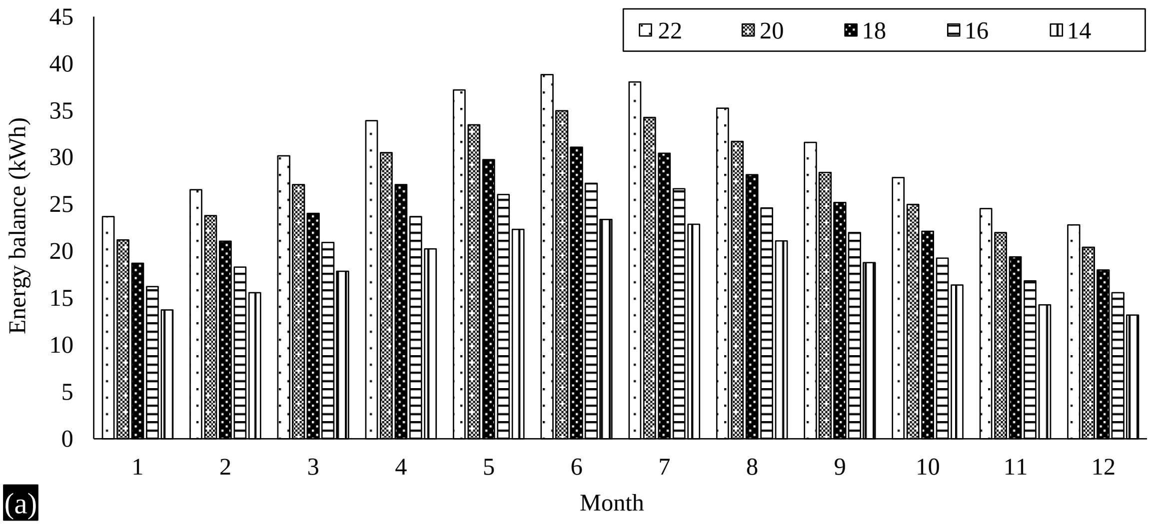

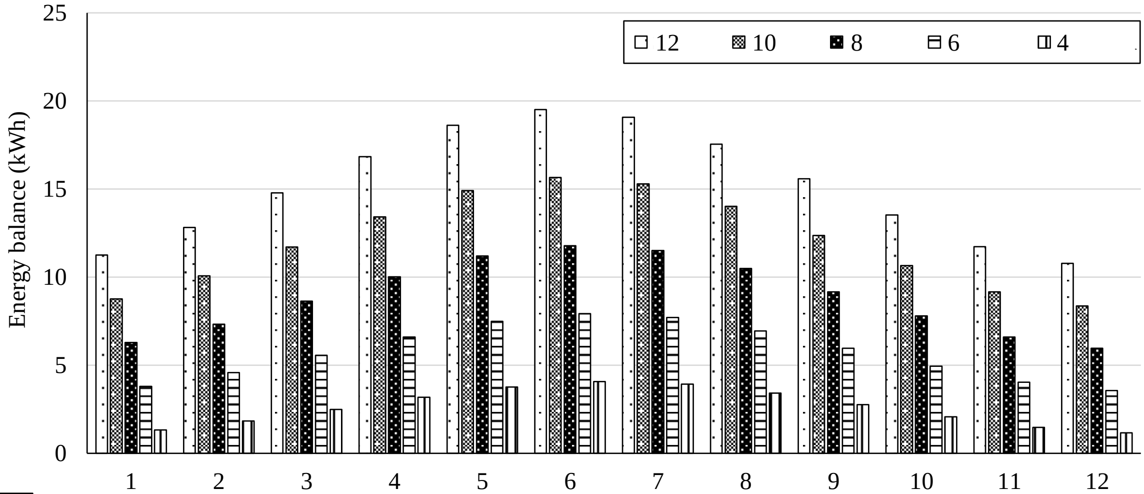

(b)

Figure 4. Monthly daily energy balance for household low energy demand and variable PV panel configuration ((a) 22 to 14 panels; (b) 12 to 4 panels).

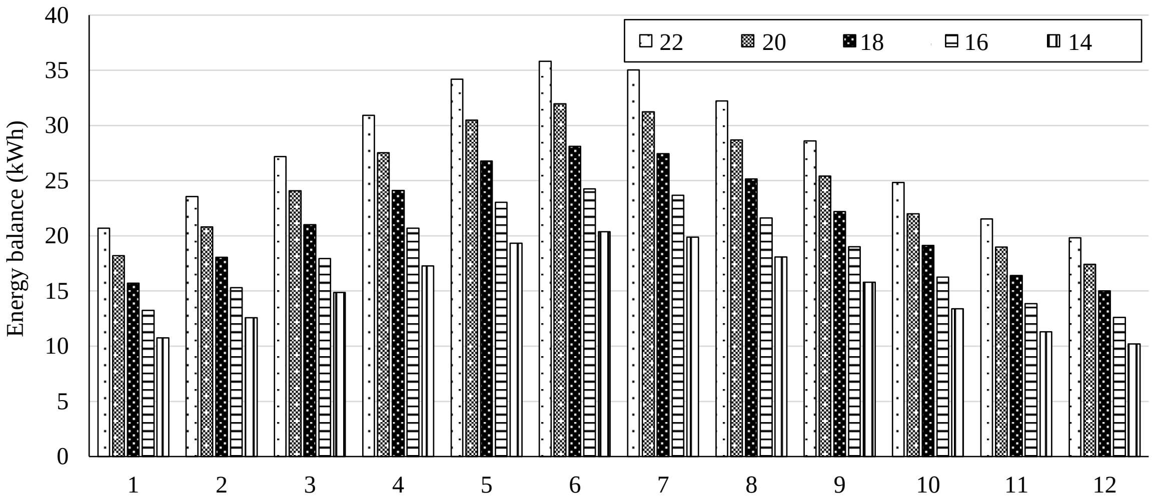

(a)

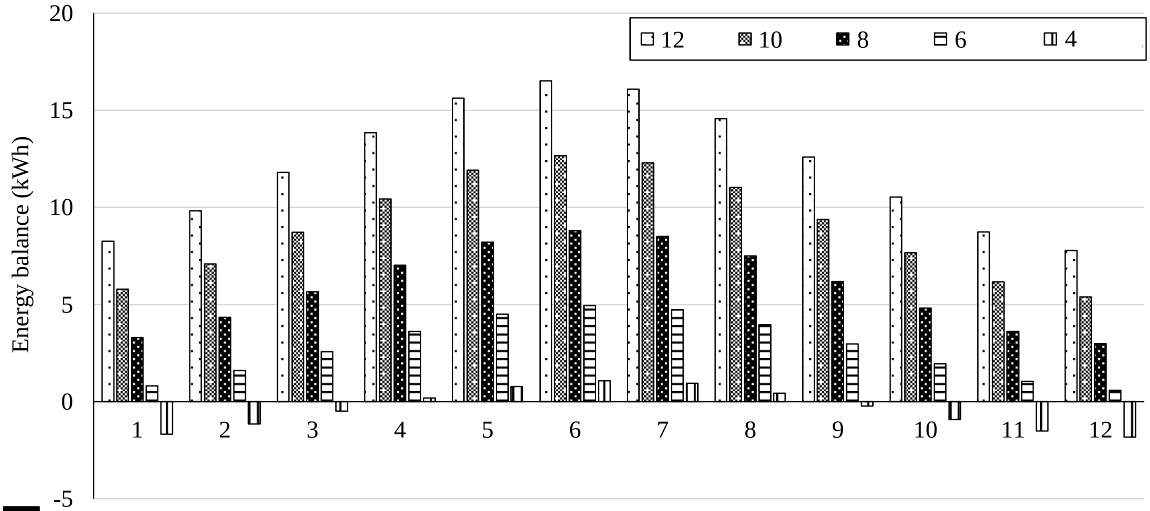

(b)

Figure 5. Monthly daily energy balance for household medium energy demand and variable PV panel configuration ((a): 22 to 14 panels; (b) 12 to 4 panels).

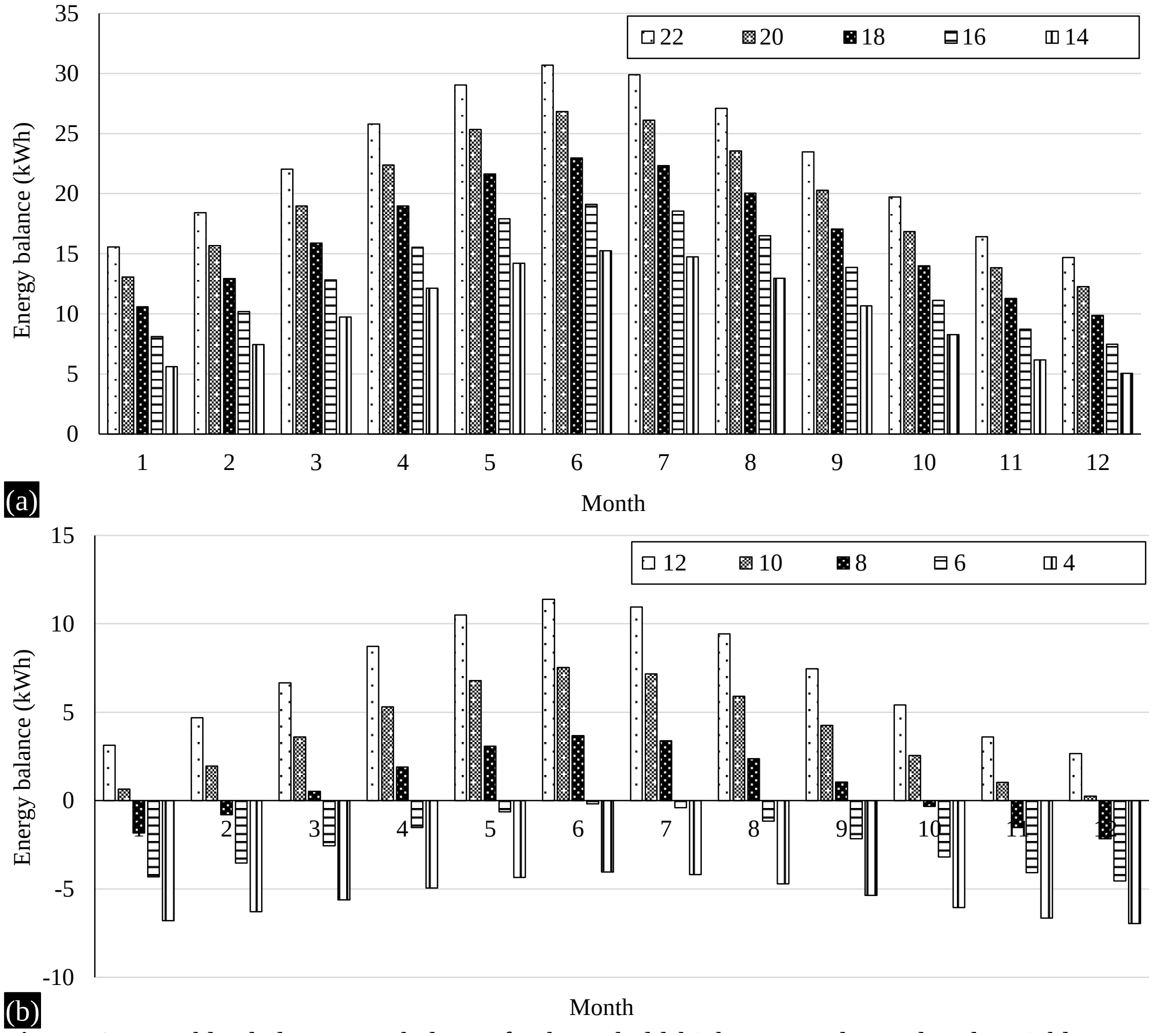

Figure 6. Monthly daily energy balance for household high energy demand and variable PV panel configuration ((a) 22 to 14 panels; (b) 12 to 4 panels).

We split the energy balance evaluation for each household energy demand level into two graphs to make the reading more comfortable. The bar distribution for every group runs from the highest to the lowest number of PV panels.

We realize that for low energy demand levels, all PV configurations exhibit a positive energy balance, which makes them suitable for hydrogen storage systems. A similar analysis applies to the medium level, except for the case of the 4 PV panels configuration, where a negative energy balance occurs, making the hydrogen storage unit non-feasible. Finally, for high energy demand levels, from the eight PV panel configurations, the hydrogen storage system is nonsense because of the negative energy balance. The calculated energy balance neglects electric wiring power losses from PV panels to household mainframes because of its low value (<1%).

Storage System

The principal storage system characteristic is the pressure of the hydrogen storage tank. We can accumulate as much hydrogen as is produced from the energy balance until the pressure limit is reached. Because the electrolyzer operates at an efficiency of 75%, we determined the hydrogen production using the following expression:

$$m_{H_2} = \eta_{ely} \left(\frac{\xi_{bal}}{\xi_{ely}} \right) \tag{26}$$

ISSN: 2249-863X (Online), ISSN: 2321-4244 (Print)

Applying Equations (4) and (26) we obtain to the energy balance data from Figures 4–6.

The missing bars corresponding to four panels and 4–6 panels PV configuration in medium and high energy demand levels are due to the negative energy balance; therefore, no hydrogen production is feasible. The hydrogen produced is compressed in the storage tank at a pressure given by the following expression:

$$P = \frac{m_{H_2}}{\rho_{H_2} V_{tk}} \quad (27)$$

For a tank of 150 liters, the current size for the semi-detached and detached houses is as follows.

Analyzing the tank pressure values shown in Figures 10–12, we realize that the compressor operates in the 0-70 bars range, which is compatible with many models in the market. The associated energy for hydrogen compression is derived from Equation (21), and considering hydrogen as an ideal gas, we have:

$$W_{comp} = \frac{1}{\eta_{comp}} V_{tk} \Delta P \quad (28)$$

The compressor efficiency depends on the pressure gain, compressor type, and fluid; therefore, we operated with the standard average value for the air compressor, which is the most currently used, and a maximum pressure gain of 70 bars, corresponding to the upper limit in our simulation. In this case, the estimated value was 77% [31].

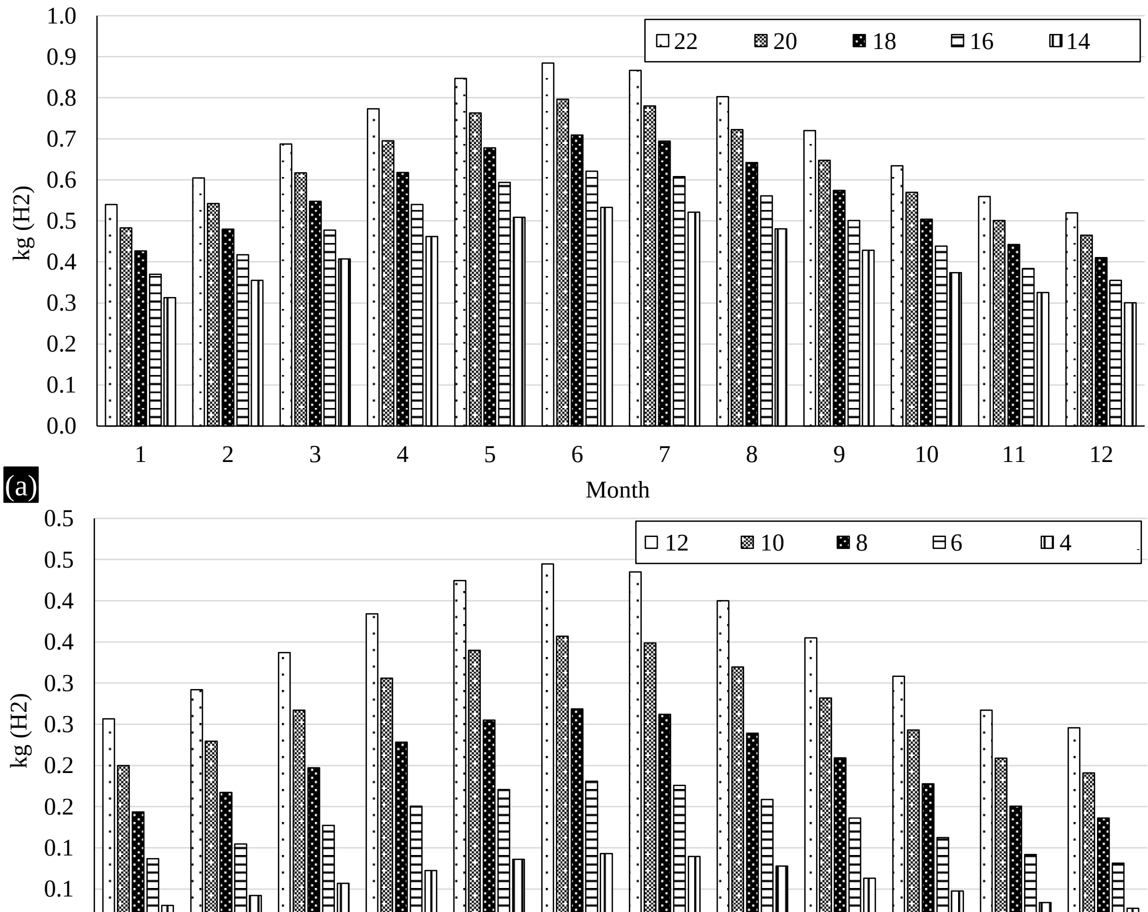

Figure 7. Monthly daily hydrogen production for household low energy demand and variable PV panel configuration ((a) 22 to 14 panels; (b) 12 to 4 panels).

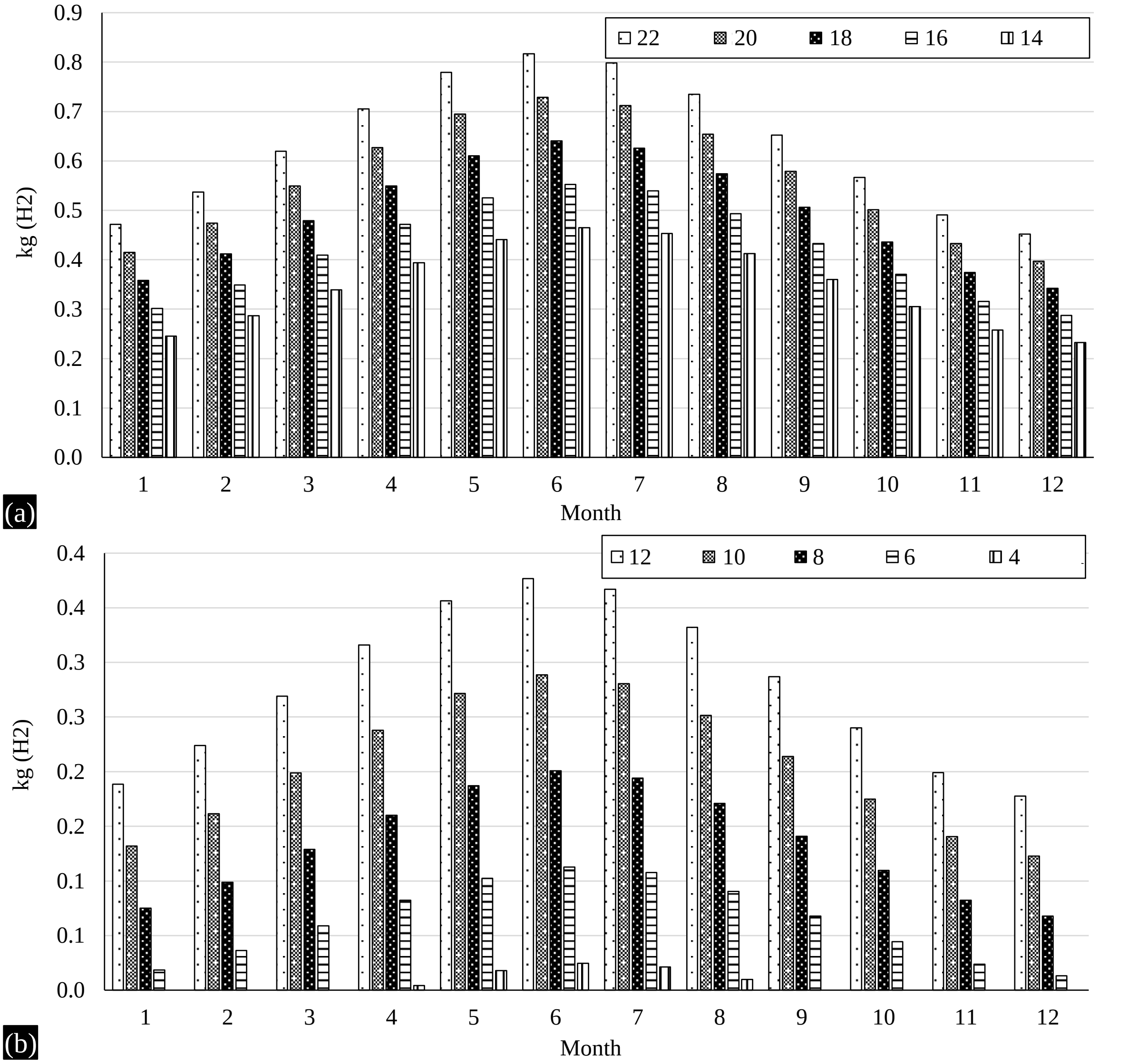

Figure 8. Monthly daily hydrogen production for household medium energy demand and variable PV panel configuration ((a) 22 to 14 panels; (b) 12 to 6 panels).

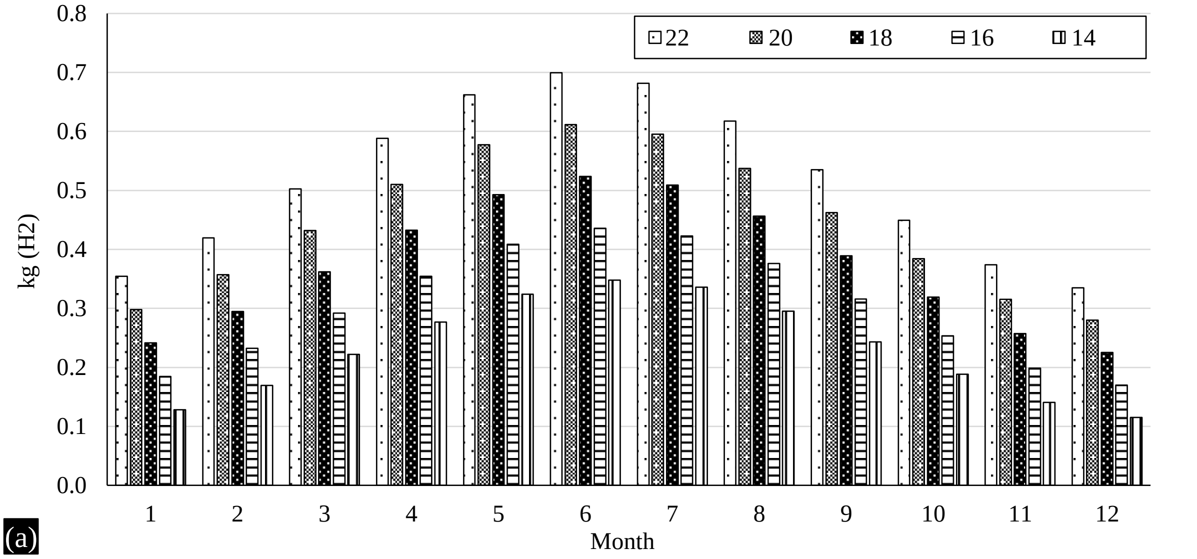

Journal of Power Electronics & Power Systems
Volume 14, Issue 3
ISSN: 2249-863X (Online), ISSN: 2321-4244 (Print)

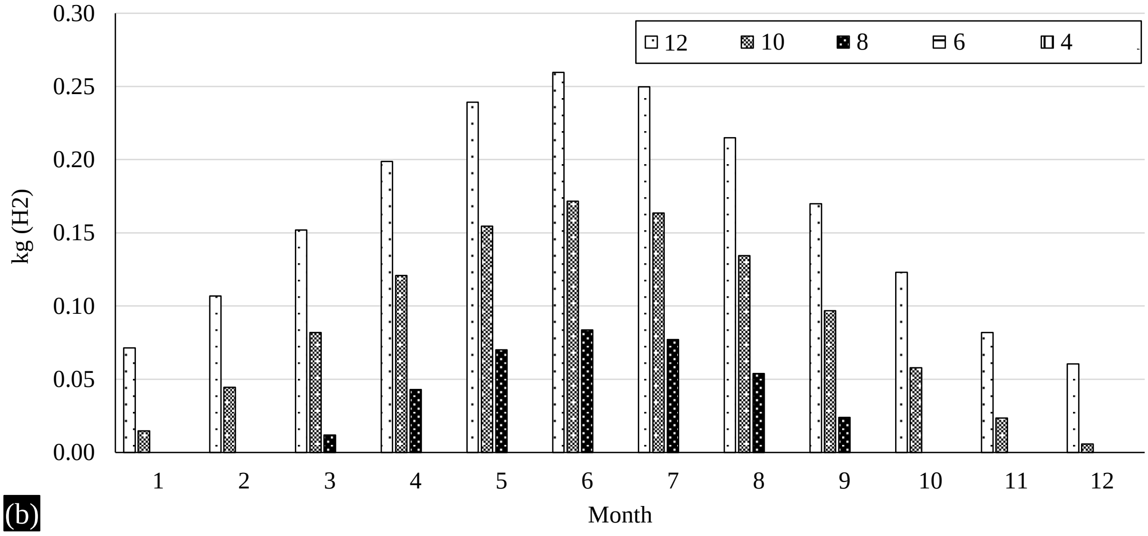

(b)

Figure 9. Monthly daily hydrogen production for household high energy demand and variable PV panel configuration ((a) 22 to 14 panels; (b) 12 to 8 panels).

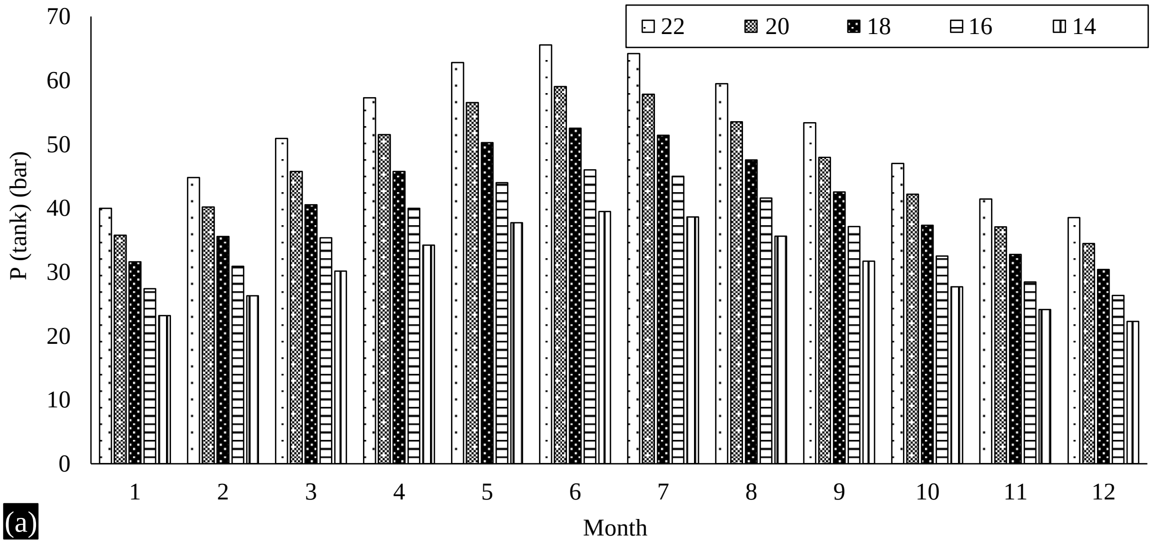

(a)

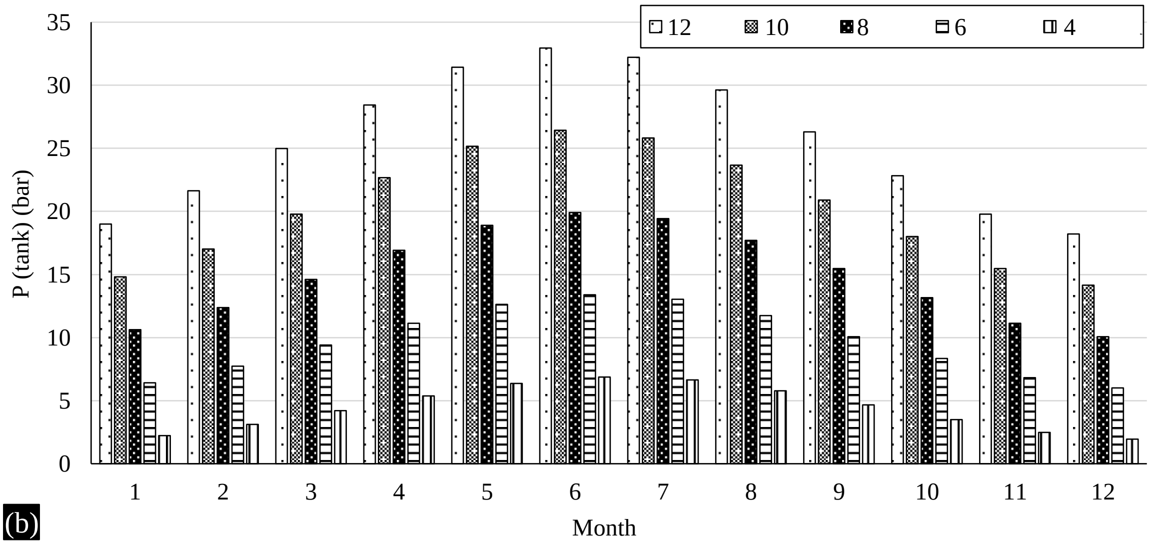

(b)

Figure 10. Hydrogen storage tank pressure for household low energy demand and variable PV panel configuration ((a) 22 to 14 panels; (b) 12 to 4 panels).

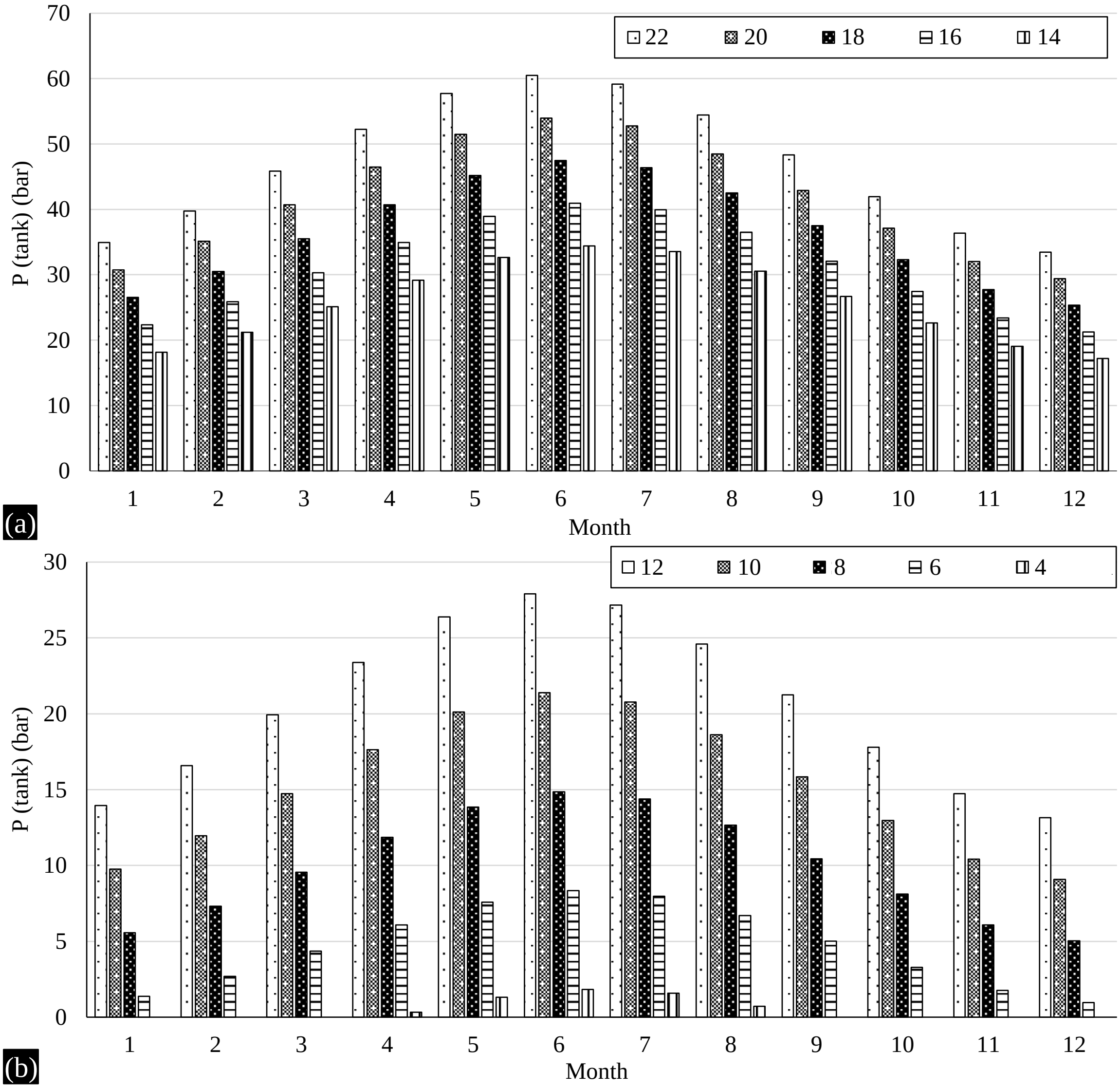

Figure 11. Hydrogen storage tank pressure for household medium energy demand and variable PV panel configuration ((a) 22 to 14 panels; (b) 12 to 6 panels).

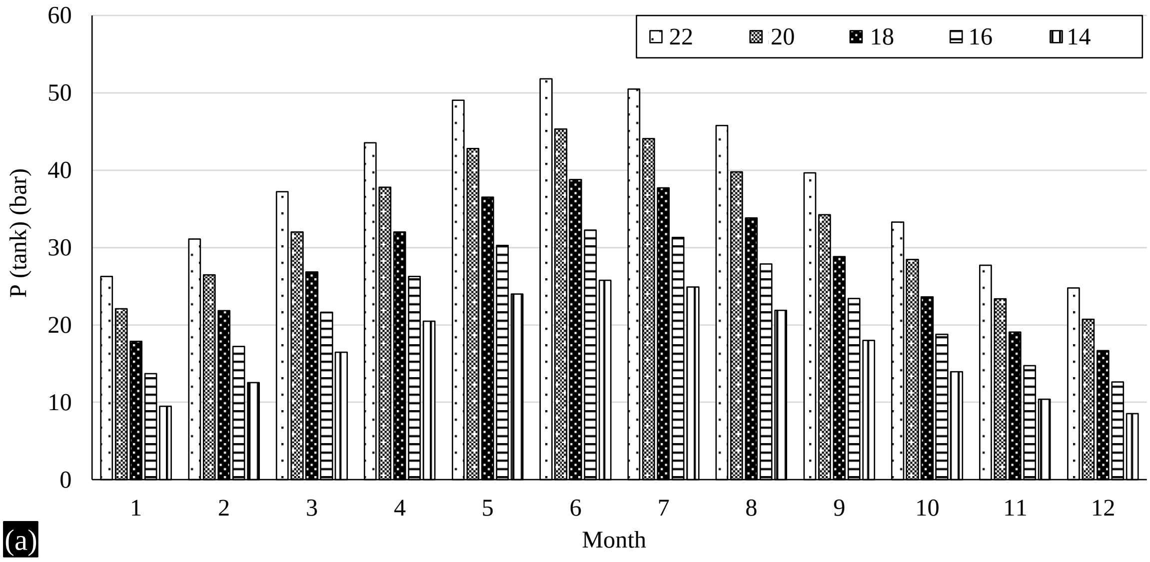

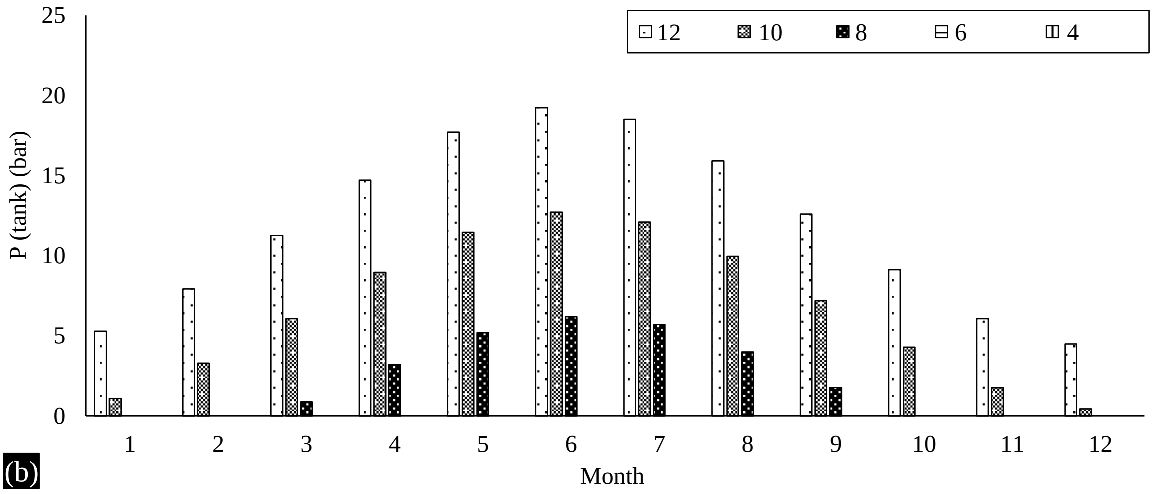

(b)

Figure 12. Hydrogen storage tank pressure for household high energy demand and variable PV panel configuration ((a) 22 to 14 panels; (b) 12 to 8 panels).

Hydrogen compressor energy consumption is important; however, the ratio of this energy to the PV generation represents a more significant parameter to understand the influence of hydrogen compression on the energy balance; therefore, combining Equations (25) and (28), we have.

$$\frac{W_{comp}}{\xi_{FV}} = \frac{V_{tk}\Delta P}{\eta_{comp}\eta_{conv}^{DC-AC}\eta_{conv}^{AC-DC} N P_{FV}(psh) f_{\gamma}} \quad (29)$$

Now, applying data from our prototype, we obtain:

$$\frac{W_{comp}}{\xi_{FV}} = 0.018 \quad (30)$$

This value represents less than 2% of the energy generated. Therefore, we consider that the hydrogen compression process barely affects the global energy performance of the installation.

HYDROGEN STORAGE SYSTEM ANALYSIS

The simulation analysis shows the viability of the proposed system with coherent results that are compatible with the standard household characteristics. The simulation proved that hydrogen storage is feasible and guarantees self-consumption installation with a daily null or positive energy balance, avoiding dependence on the grid.

Compared to battery storage systems, hydrogen storage has advantages and drawbacks, which are summarized in Table 3. The comparative analysis of the advantages and drawbacks of battery and hydrogen storage systems can tip the balance towards one or the other depending on the objectives pursued. For household installation with a PV power source, a flexible capacity to adapt to variable power generation is critical, especially in off-grid conditions, because the variability in solar radiation, and thus in electric energy generation, may result in overproduction, which a battery cannot absorb. The hydrogen storage system, however, can absorb all the excess energy within the limits imposed by the maximum pressure supported by the storage tank.

Table 3. Advantages and drawbacks of hydrogen storage system [32–35].

Advantages	Drawbacks
Higher power and energy density	Higher price
Longer autonomy	More complex design
Higher storage capacity	Higher maintenance costs
Adaptive capacity to variable energy excess	Larger room
Lower self-discharge	Higher security measurements
Lower environmental impact	Additional elements

ECONOMIC ASSESSMENT

Because the proposed system involves new elements, we evaluated the investment and maintenance costs compared to a conventional system using batteries as storage units. Analyzing the layout in Figure 2, we can establish the differential elements between our design and the conventional design (Table 4).

The current design requires higher investment because of the many additional elements; however, because the batteries are expensive, especially lithium-ion technology, the installation cost is similar. Table 5 presents the average prices of the components listed in Table 4.

On-grid installations do not suffer from this problem because the excess energy that the battery does not absorb can be injected into the grid, avoiding battery overcharging. Hydrogen storage systems can inject electric energy into the grid or export hydrogen overproduction to external facilities, showing higher flexibility, which could make them more attractive. Concerning the safety measurements for hydrogen handling and storage, we refer to specialized literature, which describes hydrogen production, transmission, distribution, and storage [36–39].

Comparing the N and C element prices, we realize that the conventional design is more expensive, with 5268€ ($5742) versus 2500€ ($2725) for a month's battery storage capacity. If we match the new and conventional design prices, we should reduce the battery capacity by half, allowing only two weeks of autonomy.

CONCLUSIONS

A hydrogen storage system for household installations is feasible, as shown in the simulation run in this study. This system is compatible with standard on-grid and autonomous household installations. We tested the system for low-, medium-, and high-energy demand levels for PV panel variable numbers. The test results show that some configurations with high energy demand and a low number of PV panels are incompatible with hydrogen storage systems because of the daily average negative energy balance.

Table 4. Differential elements between the current design and conventional system.

Current design	Conventional system
Distilled water tank Electrolyzer Pump Compressor Water container Hydrogen tank Valves	Battery block

Table 5. Differential elements between the current design and conventional system.

Element	Average cost (€/$)
Distilled water tank (N)	22.00/23.98
Electrolyzer (N)	575.22/627.00
Pump (N)	33.02/36.00
Compressor (N)	205.50/224.00
Water container (N)	84.20/160.00
Hydrogen tank (N)	1100.90/1200.00
Valves (N)	52.00/56.68
Hydrogen burner	426.60/465.00
Battery block Li-ion (C)	5412/5900
Battery block Lead-acid (C)	5124/5585

The type (N) corresponds to the new design and (C) to the conventional one.

The simulation proves that the hydrogen storage system can absorb excess energy from the PV panel generation under variable solar radiation. The simulation was run for a household prototype with characteristics similar to those of a conventional semi-detached or detached house.

The simulation results show a storage pressure range of 0–70 bar, which is compatible with most mid-range commercial air compressors. The electrolyzer for hydrogen production and the fuel cell for electricity generation are also compatible with commercial standards for a low-power range.

The proposed technology provides an alternative to the battery storage system with higher flexibility and adaptive capacity under variable operating conditions, especially in off-grid installations where battery storage may not be able to absorb all the excess energy generated, leading to an overload that damages the storage system or releases the excess energy in the form of heat, which significantly reduces the efficiency of the system.

The new system is economically viable and saves money compared with the conventional system, with a 50% investment reduction. The traditional system can match the cost by reducing the battery capacity; therefore, the energy storage autonomy is reduced by half.

REFERENCES

1. Luthander R, Widén J, Nilsson D, Palm J. Photovoltaic self-consumption in buildings: A review. Appl Energy. 2015;142:80–94. DOI: 10.1016/j.apenergy.2014.12.028.
2. Wegertseder P, Lund P, Mikkola J, García Alvarado RG. Combining solar resource mapping and energy system integration methods for realistic valuation of urban solar energy potential. Sol Energy. 2016;135:325–36. DOI: 10.1016/j.solener.2016.05.061.
3. Ciocia A, Amato A, Di Leo P, Fichera S, Malgaroli G, Spertino F, Tzanova S. Self-consumption and self-sufficiency in photovoltaic systems: Effect of grid limitation and storage installation. Energies. 2021;14:1591. DOI: 10.3390/en14061591.
4. Mulder G, De Ridder FD, Six D. Electricity storage for grid-connected household dwellings with PV panels. Sol Energy. 2010;84:1284–93. DOI: 10.1016/j.solener.2010.04.005.
5. Mishra PP, Latif A, Emmanuel M, Shi Y, McKenna K, Smith K, Nagarajan A. Analysis of degradation in residential battery energy storage systems for rate-based use-cases. Appl Energy. 2020;264:114632. DOI: 10.1016/j.apenergy.2020.114632.
6. Wang S, Guo D, Han X, Lu L, Sun K, Li W, Sauer DU, Ouyang M. Impact of battery degradation models on energy management of a grid-connected DC microgrid. Energy. 2020;207:118228. DOI: 10.1016/j.energy.2020.118228.
7. Podder A. (2021). Batteries for Affordable Housing: Key Trends, Barriers, and Opportunities. [online] BatteryBits Editors. Medium. Available from: https://medium.com/batterybits/batteries-for-affordable-housing-f9073f0fdee3.
8. Ardani K. (2017). How Much Does a Rooftop Solar System With Batteries Cost? [online] Greentechmedia.com. Available from: https://www.greentechmedia.com/articles/read/How-Much-Does-a-Rooftop-Solar-System-With-Batteries-Cost
9. Endesa (2023). Virtual battery and solar self-consumption. [online] Endesa. Available from: https://www.endesa.com/en/blogs/endesa-s-blog/light/virtual-battery-solar-self-consumption.
10. Liu J, Hu H, Yu SS, Trinh H. Virtual power plant with renewable energy sources and energy storage systems for sustainable power grid-formation, control techniques and demand response. Energies. 2023;16:3705. DOI: 10.3390/en16093705.
11. Energy Nordic. (2023). What is virtual battery - Energy Nordic. [online] Energy Nordic. Available from: https://energynordic.com/solar-energy/what-is-virtual-solar-battery/
12. European Commission. Best practices on renewable energy self-consumption [Internet]. Brussels: Commission Staff Working Document; 2015 Jul 15. Report No.: SWD(2015) 141 final. Available from: https://eur-lex.europa.eu/legal-content/EN/TXT/PDF/?uri=CELEX:52015SC0141

13. Ge P, Hu Q, Wu Q, Dou X, Wu Z, Ding Y. Increasing operational flexibility of integrated energy systems by introducing power to hydrogen. IET Renew Power Gener. 2020;14:372–80. DOI: 10.1049/iet-rpg.2019.0663.
14. Hwang HT, Varma A. Hydrogen storage for fuel cell vehicles. Curr Opin Chem Eng. 2014;5:42–8. DOI: 10.1016/j.coche.2014.04.004.
15. Muthukumar P, Kumar A, Afzal M, Bhogilla S, Sharma P, Parida A, et al. Review on large-scale hydrogen storage systems for better sustainability. Int J Hydrogen Energy. 2023.
16. Blain L. (2021). World-first home hydrogen battery stores 3x the energy of a Powerwall 2. [online] New Atlas. Available from: https://newatlas.com/energy/lavo-home-hydrogen-battery-storage/
17. Enhkardt S. (2021). World-first home hydrogen battery stores 3x the energy of a Powerwall 2. [online] New Atlas. Available from: https://newatlas.com/energy/lavo-home-hydrogen-battery-storage/
18. Hollmuller P, Joubert JM, Lachal B, Yvon K. Evaluation of a 5 kWp photovoltaic hydrogen production and storage installation for a residential home in Switzerland. Int J Hydrogen Energy. 2000;25:97–109. DOI: 10.1016/S0360-3199(99)00015-4.
19. Navas SJ, Cabello González GM, Pino FJ. Hybrid power-heat microgrid solution using hydrogen as an energy vector for residential houses in Spain. A case study. Energy Convers Manag. 2022;263:115724. DOI: 10.1016/j.enconman.2022.115724.
20. Aneke M, Wang M. Energy storage technologies and real life applications–A state of the art review. Appl Energy. 2016;179:350–77. DOI: 10.1016/j.apenergy.2016.06.097.
21. Green DW, Perry RH, editors. Perry's Chemical Engineers' Handbook. 8th ed. New York: McGraw-Hill; 2008.
22. Azizan MT, Aqsha A, Ameen M, Syuhada A, Klaus H, Abidin SZ, Sher F. Catalytic reforming of oxygenated hydrocarbons for the hydrogen production: an outlook. Biomass Convers Biorefin. 2020;1–24. DOI: 10.1007/s13399-020-01081-6. PubMed: 33110738.
23. Brown LL. Van Nostrand's encyclopedia of chemistry. Am J Pharm Educ. 2005;562:1–5.
24. Al Oweidi KF, Jamshed W, Goud BS, Ullah I, Usman, Mohamed Isa SSP, El Din SM, Guedri K, Jaleel RA. Partial differential equations modeling of thermal transportation in Casson nanofluid flow with Arrhenius activation energy and irreversibility processes. Sci Rep. 2022;12:20597. DOI: 10.1038/s41598-022. PubMed: 36446992.
25. Bourges B, editor. Climatic data handbook for Europe. Climatic data for the design of solar energy systems. Commission of the European Communities. DG XII. Dordrecht: Kluwer Academic Publishers; 1992 Apr 30.
26. Armenta-Déu C, Arenas J. Efficiency improvement in aerothermal household heating systems. J Refrig Air Cond Heat Vent. 2023;10(3):1–15.
27. Duffie JA, Beckman WA. Solar Engineering of Thermal Processes. 4th ed. Hoboken: John Wiley & Sons; 2013.
28. Azzurro ZCS. (2024). 1PH 3000TLM-V1/1PH 6000TLM-V1 – Plus series single-phase chain inverter [online]. Available from: https://www.zcsazzurro.com/inverter/azzurro-single-phase-string-inverter-plus-series-1ph-3000tlm-v1-1ph-6000tlm-v1
29. Victron. (2024). Multiplus C12-3000-80 inverter/charger [online]. Available from: https://www.victronenergy.com/inverters-chargers/multiplus-12v-24v-48v-800va-3kva.
30. Ziegler MS, Trancik JE. Re-examining rates of lithium-ion battery technology improvement and cost decline. Energy Environ Sci. 2021;14(4):1635–51. DOI: 10.1039/D0EE02681F.
31. Renardson A. (2024). A Guide To Air Compressor Efficiency. Air Supply. [online] Air Supply UK. Available from: https://www.airsupply.co.uk/blogs/a-guide-to-air-compressor-efficiency-how-to-calculate-and-maximise-efficiency/
32. Usman MR. Hydrogen storage methods: Review and current status. Renew Sustain Energy Rev. 2022;167:112743. DOI: 10.1016/j.rser.2022.112743.
33. Eberle U, Felderhoff M, Schüth F. Chemical and physical solutions for hydrogen storage. Angew Chem Int Ed Engl. 2009;48:6608–30. DOI: 10.1002/anie.200806293. PubMed: 19598190.

34. Züttel A. Hydrogen storage methods. Naturwissenschaften. 2004;91:157–72. DOI: 10.1007/s00114-004-0516-x. PubMed: 15085273.
35. Hirose K. Handbook of Hydrogen Storage: New Materials for Future Energy Storage. Chichester, UK: John Wiley & Sons; 2010
36. H2tools. (2024). Hydrogen safety checklist [online]. Available from: https://h2tools.org/sites/default/files/HydrogenSafetyChecklist.pdf.
37. Li H, Cao X, Liu Y, Shao Y, Nan Z, Teng L, Peng W, Bian J. Safety of hydrogen storage and transportation: An overview on mechanisms, techniques, and challenges. Energy Rep. 2022;8:6258–69. DOI: 10.1016/j.egyr.2022.04.067.
38. Moradi R, Groth KM. Hydrogen storage and delivery: Review of the state of the art technologies and risk and reliability analysis. Int J Hydrogen Energy. 2019;44(23):12254–69. DOI: 10.1016/j.ijhydene.2019.03.041.
39. Barthélémy H, Weber M, Barbier F. Hydrogen storage: Recent improvements and industrial perspectives. Int J Hydrogen Energy. 2017;42(11):7254–62. DOI: 10.1016/j.ijhydene.2016.03.178.

